

Georadar processing and imaging with Gabor deconvolution – University of Houston Coastal Center

Adrian D. Smith¹, Robert J. Ferguson¹, and Robert R. Stewart².

1. University of Calgary, CREWES

2. University of Houston, CREWES

Summary

A georadar (GPR) dataset collected at the University of Houston Coastal Center (UHCC) in 2010 and 2012 contains a 2D line passing over a series of culverts. We process it using a Gabor deconvolution workflow instead of traditional processing methods. We find that Gabor deconvolution corrects for attenuation and greatly improves resolution and signal bandwidth at late arrival times. Diffractor imaging velocities are estimated by diffraction hyperbola fitting and the line is imaged using zero-offset (ZO) Gazdag migration to collapse the hyperbolic events on the section. We also use shot-record Gazdag prestack depth migration (PSDM) to give an improved image. As our subsurface geometry is circular, we apply a correction factor to the diffractor velocity to obtain a more accurate image after migration. Certain features are visible in the deconvolved section, possibly including the steeply dipping flanks of the edge of the bridge. In the future we hope to refine our velocity model to take into account lateral velocity variations, and process and image the other three surveys in the dataset.

Introduction

The sitemap for a georadar (GPR) dataset acquired at the University of Houston Coastal Center (UHCC) located near La Marque Texas, United States is given in Figure 1. The acquisition consists of four surveys; a 3D grid in 2010 and three 2D lines in 2012 (Figure 1, Table 1). The data were acquired using a bistatic time-domain georadar system with transmitter-receiver antenna separations given in Table 1.

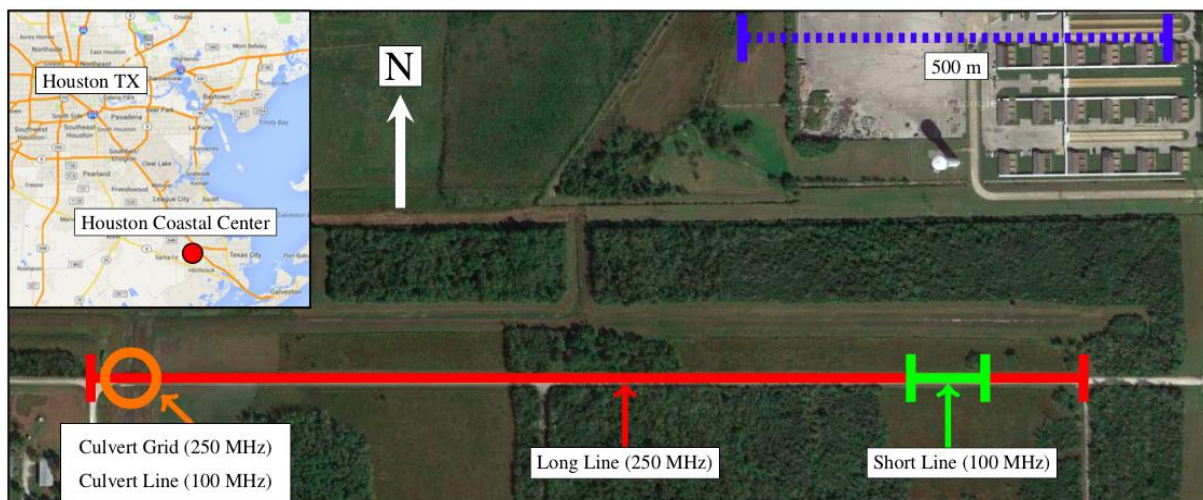


Figure 1: Site map of the UHCC. The approximate locations of the four georadar surveys on-site are highlighted. The parameters for each individual survey are shown in Table 1. *Satellite imagery courtesy of Google Maps 2014.*

	Culvert Grid	Culvert Line	Long Line	Short Line
Antenna Frequency	250 MHz	100 MHz	250 MHz	100 MHz
Step Size (m)	0.05	0.1	0.05	0.1
Sample Rate (ns)	0.4	0.8	0.4	0.8
Antenna Separation (m)	0.27	0.50	0.27	0.50

Table 1: Parameters of the four UHCC georadar surveys. Their locations are shown in Figure 1.

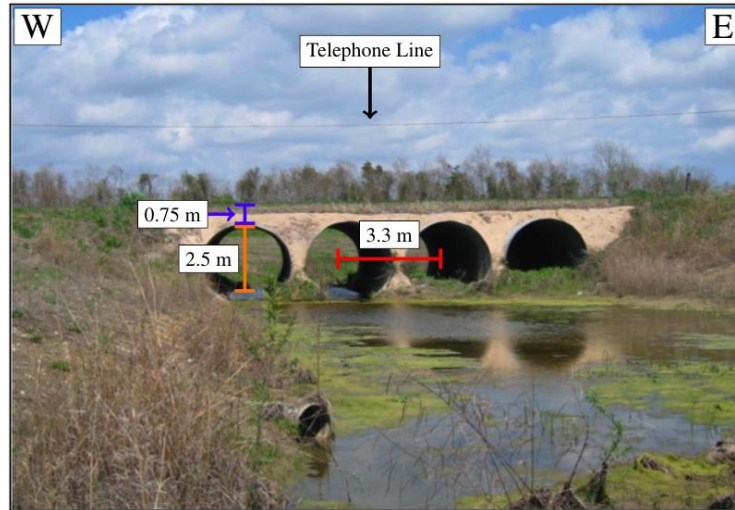


Figure 2: Cross-sectional view of the culverts at the UHCC. All distances are approximate. Modified from Aziz et al. (2013).

There is a series of four culverts supporting a road crossing a bayou on the western edge of the site (Figures 1 and 2). They are made of corrugated steel pipe coated with zinc-galvanized aluminium and are highly conductive. A mixture of crushed limestone and oyster shells covers the first 15 cm of the top of the surface road and a stabilizer sand was used to fill the remaining space to the top of the culverts (Figure 2, Aziz et al. (2013)). We discuss our work on the 2D Culvert Line exclusively.

Seismic-Based Gabor Nonstationary Deconvolution Processing

It has been shown in previous work that seismic-based georadar processing workflows incorporating Gabor nonstationary deconvolution as summarized in Margrave et al., 2011 are superior to more traditional processing flows (Ferguson et al., 2012). Gabor deconvolution provides better results due to its ability to account for both a highly nonstationary wavelet as well as Q attenuation, which is about an order of magnitude smaller (resulting in a larger attenuation effect) than with seismic data (Ferguson and Margrave, 2012). We apply the Gabor deconvolution processing flow in Table 2 to the Culvert Line from the UHCC dataset. We find that application of the mute gives poorer results than without and so decide to exclude it. Figure 3 shows the Culvert Line after conventional Wiener spiking deconvolution processing and Figure 4 after application of Gabor deconvolution processing. The Gabor deconvolved section is both much better focused and has more visible reflection energy deeper in the section than the section after a spiking decon.

Process	Parameters
(1) Time Zero	8 ns shift
(2) Top Mute	0 – 13 ns
(3) Gabor Deconvolution	(<i>gabordecon</i> from the CREWES processing toolbox) $t_{\text{win}} = 10/f_{\text{Nyq}}$, $t_{\text{inc}} = 1/2f_{\text{Nyq}}$, $t_{\text{smo}} = 50/f_{\text{Nyq}}$, $f_{\text{smo}} = 87$ MHz, Hyperbolic smoothing, $\text{stab} = 0$, Minimum phase, Synthesis window is unity, $\text{gbd} = 60$
(4) Bandpass Filter	$0.05f_{\text{Nyq}} - 0.6f_{\text{Nyq}}$ (31 – 375) MHz

Table 2: Seismic-based Gabor deconvolution processing parameters based on the workflow developed in Ferguson et al. (2012). f_{Nyq} is the Nyquist frequency of the data, which is 625 MHz for the Culvert Line.

Seismic-Based Gabor Deconvolution Results

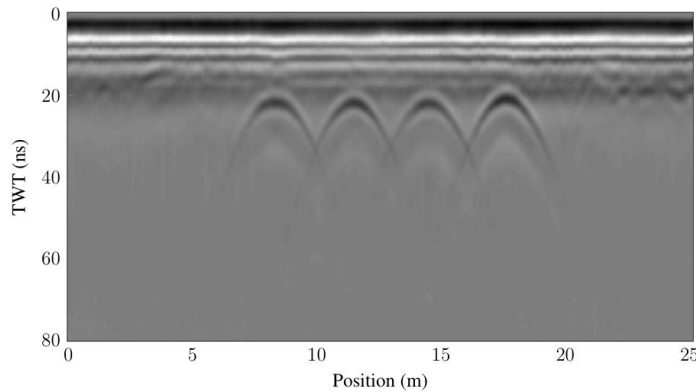


Figure 3: Wiener spiking deconvolved Culvert Line after bandpass filtering. No top mute applied prior to decon.

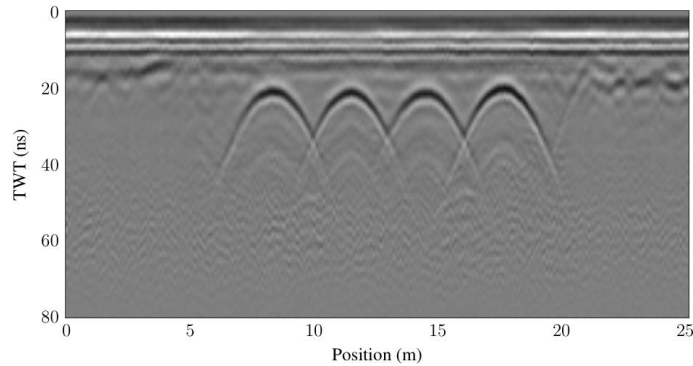


Figure 4: Gabor deconvolved Culvert Line after bandpass filtering. No top mute applied prior to decon.

Imaging

We perform depth migrations of the processed georadar record from the Culvert Line. First, we fit hyperbolae to the culvert reflection signatures to obtain velocities that collapsed the signatures to diffraction points under migration. We generate a constant velocity model using these diffractor velocities and depth image using both zero-offset (ZO) Gazdag migration (Figure 5) and shot-record Gazdag prestack depth migration (PSDM) (Figure 6). We observe better results using shot-record migration. The diffraction energy is better collapsed and the section up shallow above the culverts is much better focused in the PSDM section (Figure 6) vs. the ZO migrated section in Figure 5 as it takes into account transmitter-receiver offset. Using a geometric velocity factor (Smith and Ferguson 2014), we reimage the data using PSDM (Figure 7). This result is a more accurate image of the subsurface, as the velocity used to image is closer to the true velocity as opposed to the diffractor velocity.

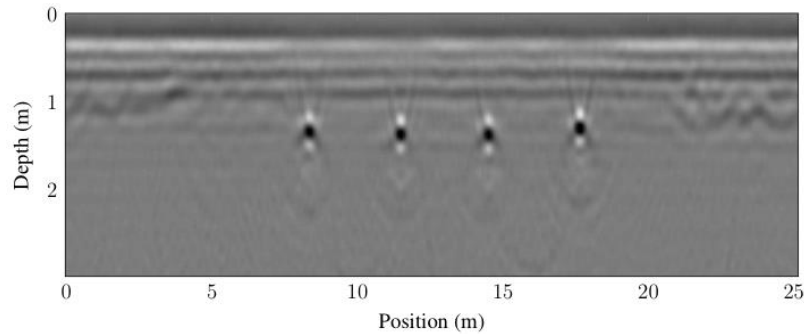


Figure 5: ZO Gazdag migrated section, using a constant velocity of 0.127 m/ns determined from diffraction hyperbola fitting. 3X vertical exaggeration.

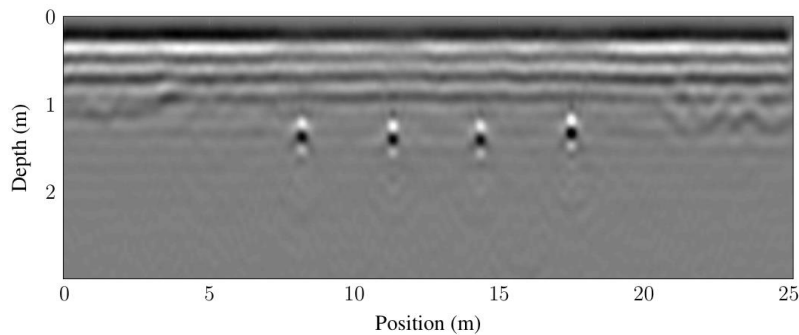


Figure 6: Shot-record Gazdag PSDM section, migrated using a constant velocity of 0.127 m/ns determined from diffraction hyperbola fitting. 3X vertical exaggeration.

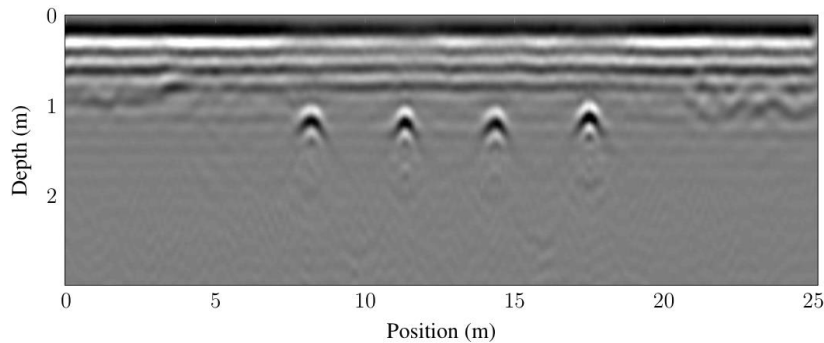


Figure 7: Shot-record Gazdag PSDM section, migrated using a constant velocity model corrected for circular geometry of 0.110 m/ns. 3X vertical exaggeration.

Conclusions

We demonstrate the superiority of Gabor deconvolution to Wiener spiking deconvolution on real 2D georadar data. Shot-record migration is superior to ZO migration and gives a more focused image. We feel that Gabor deconvolution-based processing holds great promise for generating higher quality georadar images.

Acknowledgements

The authors would like to thank to CREWES sponsors for their financial support as well as the UHCC for making the data available.

References

- Aziz, A. A., Stewart, R. R., and Green, S. L., 2013, Imaging buried culverts using ground penetrating radar: Comparing 100 MHz through 1 GHz antennae: AGU Fall Meeting Abstracts, A1.
- Ferguson, R. J., Ercoli, M., and Frigeri, A., 2012, Georadar data processing and imaging: paleoseismicity in the Piano di Castelluccio Basin, central Italy: CREWES Research Report, 24.
- Ferguson, R. J., and Margrave, G. F., 2012, Attenuation compensation for georadar data by Gabor deconvolution: CREWES Research Report, 24.
- Gazdag, J., 1978, Wave equation migration with the phase-shift method: *Geophysics*, 43, No. 7, 1342-1351.
- Margrave, G. F., Lamoureux, M. P., and Henley, D. C., 2011, Gabor deconvolution: Estimating reflectivity by nonstationary deconvolution of seismic data: *Geophysics*, 76, No. 3, W15–W30.
- Smith, A. D., and Ferguson, R. J., 2014, Geometrical corrections for poststack imaging focusing velocity analysis: CREWES Research Report, 26.
- Smith, A. D., Ferguson, R. J., and Stewart, R. R., 2014, Georadar processing and imaging with Gabor deconvolution - Houston Coastal Center: CREWES Research Report, 26.